THE JOURNAL OF BIOLOGICAL CHEMISTRY VOL. 286, NO. 23, pp. 20970–20976, June 10, 2011
© 2011 by The American Society for Biochemistry and Molecular Biology, Inc. Printed in the U.S.A.

Potential Relation of Aberrant Proteolysis of Human Protein Tyrosine Kinase 7 (PTK7) *chuzhoi* by Membrane Type 1 Matrix Metalloproteinase (MT1-MMP) to Congenital Defects*

Received for publication, March 6, 2011, and in revised form, April 18, 2011 Published, JBC Papers in Press, April 25, 2011, DOI 10.1074/jbc.M111.237669

Vladislav S. Golubkov, Alexander E. Aleshin, and Alex Y. Strongin[1]

From the Cancer Research Center, Sanford-Burnham Medical Research Institute, La Jolla, California 92037

Membrane PTK7 pseudo-kinase plays an essential role in planar cell polarity and the non-canonical Wnt pathway in vertebrates. Recently, a new *N*-ethyl-*N*-nitrosourea-induced mutant named *chuzhoi* (*chz*) was isolated in mice. *chz* embryos have severe birth defects, including a defective neural tube, defective heart and lung development, and a shortened anterior-posterior body axis. The *chz* mutation was mapped to the Ala-Asn-Pro tripeptide insertion into the junction region between the fifth and the sixth Ig-like domains of PTK7. Unexpectedly, *chz* reduced membrane localization of the PTK7 protein. We hypothesized and then proved that the *chz* mutation caused an insertion of an additional membrane type 1 matrix metalloproteinase cleavage site in PTK7 and that the resulting aberrant proteolysis of *chz* affected the migratory parameters of the cells. It is likely that aberrations in the membrane type 1 matrix metalloproteinase/PTK7 axis are detrimental to cell movements that shape the body plan and that *chz* represents a novel model system for increasing our understanding of the role of proteolysis in developmental pathologies, including congenital defects.

About three of every 100 babies born in the United States have congenital abnormalities. Congenital abnormalities are ranked 34th of the top 50 causes of total death in the United States. Debilitating cardiovascular and nervous system defects jointly represent 40% of birth defects. The death toll of congenital abnormalities (0.58%) roughly equals that of stomach, skin, or oral cancers. Mechanistic research into birth defects is required to more efficiently contribute to prevention and correction of these disorders.

The canonical, β-catenin-dependent and non-canonical, β-catenin-independent Wnt signaling pathways are conserved in eukaryotes and are critical for the diverse events in embryonic development and disease. The non-canonical Wnt/planar cell polarity (PCP)[2] signaling controls cell organization within the tissue plane (1, 2). The Wnt/PCP signaling affects the actin cytoskeleton via RhoA GTPase activation through dishevelled associated activator of morphogenesis 1 (DAAM1) and dishevelled activator of morphogenesis 2 (DAAM2). The first PCP signaling events occur at a gastrulation stage of embryogenesis. These events regulate the polarized directed cell movement to accomplish convergent extension for the anterior-posterior body axis elongation, neural tube closure, and craniofacial morphogenesis (3–6). Convergent extension failure results in a shortened anterior-posterior body axis and widened lateral axis (convergent extension phenotype), a defective neural system, and craniofacial abnormalities.

Ubiquitously expressed PTK7 (also called colon carcinoma kinase-4 (CCK-4)) is a Wnt coreceptor and a regulator of PCP in vertebrates (7–13). Membrane PTK7 includes seven extracellular Ig domains, a transmembrane region, and a catalytically inert cytoplasmic tyrosine kinase (PTK) domain (8, 9, 11, 14). PTK7 is evolutionary conserved in humans and mice and also chicken klingon (KLG), *Drosophila* (Dtrk/Off-track), and hydra (Lemon) (7). It is likely that PTK7 regulates PCP and signaling via homotypic interactions between the extracellular Ig domains and via the cytoplasmic PTK domain, respectively. PTK7 can form multimers (10). PTK7 signaling can be achieved through its interactions with plexins and semaphorins, albeit the precise mechanisms are yet to be determined (15, 16). PTK7 mutant mice that expressed either a 1–114 PTK7 truncation or a cytoplasmic domain deletion died because of severe defects in neural tube closure (10).

Recently, a new *N*-ethyl-*N*-nitrosourea-induced mutant named *chuzhoi* (*chz*) was isolated and characterized in mice. *chz* mutant embryos have defective convergent extension, including a broadened midline, a shortened anterior-posterior body axis, abnormal cell polarity in the ear, and defective neural tube and heart and lung development. The cause of *chz* is the unnatural Ala-Asn-Pro insertion into the junction region between the 5th and the 6th Ig-like domains of the PTK7 ectodomain portion. We determined that the insertion, unexpectedly, significantly reduced membrane localization of the PTK7 protein (17).

Recent studies indicate that invasion-promoting MT1-MMP controls PCP in zebrafish (*Danio rerio*) development (18). MT1-MMP is a prototypic member of a membrane-anchored MMP subfamily and is distinguished from soluble MMPs by a C-terminal transmembrane domain and a cytoplasmic tail (19, 20). MT1-MMP cleaves extracellular matrix proteins, initiates the activation pathway of soluble MMPs and controls the functionality of cell adhesion and signaling receptors (21–25). Knockout of MT1-MMP has the most significant phenotype among MMP gene knockout mice: MT1-MMP knockout mice are dwarfs and die at adulthood (26). Likewise, a loss of the

* This work was supported, in whole or in part, by National Institutes of Health Grants CA83017 and CA77470 (to A. Y. S.).

[1] To whom correspondence should be addressed: Cancer Research Center, Sanford-Burnham Medical Research Institute, La Jolla, CA 92037. Tel.: 858-795-5271; Fax: 858-795-5225; E-mail: strongin@sanfordburnham.org.

[2] The abbreviations used are: PCP, planar cell polarity; PTK7, protein tyrosine kinase 7; *chz*, *chuzhoi*; MT1-MMP, membrane type-1 metalloproteinase; MMP, metalloproteinase; sPTK7, soluble PTK7.

structurally similar primordial At2-MMP induces dwarfism in *Arabidopsis* plants (27).

MT1-MMP knockdown affects PCP and directed migration of the mesodermal cells in gastrulation and craniofacial morphogenesis (18). Van Gogh-like 2, a regulator of the non-canonical Wnt pathway, colocalizes with MT1-MMP and redistributes toward the leading edge of polarized human cancer cells (18). It is likely that pericellular proteolysis and PCP converge to promote efficient directed cell migration (28).

As a result, it is not entirely surprising that PTK7 and MT1-MMP are functionally linked in eukaryotes (18, 28–30). Cellular MT1-MMP, a key proinvasive proteinase, functions as a principal PTK7 sheddase. MT1-MMP cleaves the $PKP^{621} \downarrow LI$ sequence of the seventh Ig-like domain of membrane PTK7. MT1-MMP proteolysis generates the C-terminal, membrane-tethered (50-kDa) and the N-terminal, soluble (70-kDa) PTK7 1–621 fragments. Cleavage site L622D mutation results in the PTK7 mutant that is resistant to MT1-MMP. Our analysis of the MT1-MMP/PTK7 axis suggests that a balance between the MT1-MMP activity and the membrane/soluble PTK7 species is required for the correct execution of the cell migration program in both human cancer cells and zebrafish (*D. rerio*). An abnormal balance caused defects in both zebrafish development and directional migration of tumor cells.

On the basis of these data and the protein sequence of PTK7, we then hypothesized that the Ala-Asn-Pro insertion ($QVL\underline{ANP}EK \downarrow LK^{503}$, the arrow indicates the scissile bond, the insert is underlined) introduced a consensus MMP $PXX \downarrow L$ cleavage site in the PTK7 sequence. Here, we experimentally confirmed our hypothesis and demonstrated that human *chz* exhibits an additional MT1-MMP cleavage site. It becomes now possible to suggest that the N-terminal, soluble (70-kDa) 1–621 *chz* fragment readily degrades *in vivo*. This degradation of soluble *chz* leads to the aberrant membrane/soluble PTK ratio and to the significantly modified migratory and signaling cell characteristics (17, 29).

Overall, our data, especially if combined with the results of Paudyal *el al.* (17), in mice suggest that mutational aberrations of the MT1-MMP/PTK7 axis cause the PCP abnormalities during gastrulation and birth defects in eukaryotes. Further analysis is warranted to determine whether PTK7 controls cell polarity in different contexts in the course of normal development and how mutations in PTK7 disrupt PCP in relation to disease, including birth defects in humans.

MATERIALS AND METHODS

Cells and Reagents—Human fibrosarcoma HT1080 cells and human breast carcinoma MCF7 cells were obtained from the ATCC. The cells were grown in DMEM supplemented with 10% FBS. A goat polyclonal antibody AF4499 against the N-terminal 31–199 portion of PTK7 was purchased from R&D Systems. A murine monoclonal 3G4 antibody, MAB1767, against the catalytic domain of MT1-MMP and the GM6001 hydroxamate inhibitor were from Chemicon. A murine monoclonal FLAG M2 antibody, the FLAG M2 antibody, and streptavidin-agarose beads were from Sigma. Rhotekin-Rho binding domain (RBD)-agarose beads and a RhoA monoclonal antibody, ARH01, were from Cytoskeleton. EZ-Link sulfosuccinimidyl 2-(biotinamido)-ethyl-1,3-dithiopropionate and Alexa Fluor 594-phalloidin were acquired from Pierce and Invitrogen, respectively.

Cloning and Mutagenesis—HT1080 cells with the ectopic expression of MT1-MMP (HT-MT1 cells), HT1080 cells in which MT1-MMP was transcriptionally silenced (over 90% silencing) using siRNA (HT-siMT1 cells), and the required scrambled controls were obtained and extensively characterized earlier (31–34). The C-terminally tagged (with a V5 tag) wild type and catalytically inert (E240A) mutant MT1-MMP constructs (29, 32) were used to generate the MCF7-MT1 and MCF7-E240A cells, respectively. HT1080 cells with the ectopic expression of the FLAG-tagged PTK7 constructs, including the full-length wild-type PTK7 (HT-PTK7), the uncleavable PTK7 L622D mutant (HT-L622D), and the N-terminal-soluble, 1–700 ectodomain form of PTK7 (HT-sPTK7), were obtained and characterized earlier (29). The PTK7-FLAG template was used in the PCR reactions with the following primers: forward, 5′-CGTGTCCAAGTGCTG<u>GCTAACCCA</u>GAAAAGCTCAAGTTC-3′; and reverse, 5′-GAACTTGAGCTTTTC<u>TGGGTTAGC</u>CAGCACTTGGACACG-3′ to generate the *chz* mutant sequence (the mutant sequence is underlined). The resulting *chz* construct was subcloned into the pcDNA3.1D/V5-His-TOPO directional TOPO expression vector (Invitrogen). HT1080 and MCF7 cells were stably transfected with the *chz* construct using Lipofectamine 2000 (Invitrogen) to generate HT-*chz* and MCF7-*chz* cells, respectively. Stably transfected clones were selected in the presence of G418. The expression of *chz* was validated by Western blotting with the FLAG and PTK7 antibodies.

Cell Surface Biotinylation—Cell surface proteins were biotinylated by incubating cells for 1 h on ice in PBS containing 0.1 mg/ml EZ-Link sulfosuccinimidyl 2-(biotinamido)-ethyl-1,3-dithiopropionate. Cells were lysed in 20 mM Tris-HCl, 150 mM NaCl, 1% deoxycholate, and 1% octylphenoxypolyethoxyethanol (IGEPAL) (pH 7.4), supplemented with a protease inhibitor mixture set III (Sigma), 1 mM phenylmethylsulfonyl fluoride, and 10 mM EDTA. Biotinylated proteins were precipitated from cell lysates using streptavidin-agarose beads (Sigma). Biotinylated proteins were eluted from the beads using 2× SDS sample loading buffer (125 mM Tris-HCl (pH 6.8), 4% (v/v) SDS, 0.005% bromphenol blue, 20% (v/v) glycerol, 20 mM DTT).

Immunofluorescence—Cells grown on glass coverslips were fixed for 10 min with 4% paraformaldehyde, permeabilized for 5 min with 0.1% Triton X-100, and blocked for 1 h in 1% casein. Cells were stained with a primary antibody (normally at a 1:1000 dilution), followed by a secondary antibody conjugated with Alexa Fluor 488 or Alexa Fluor 594 (Molecular Probes, dilution 1:500). The coverslips were mounted in Vectashield mounting medium with DAPI (Vector Laboratories). Images were acquired using an Olympus BX51 fluorescence microscope equipped with a MagnaFire digital camera (Olympus).

Rho Activation Assay—The Rho activation assay kit (Cytoskeleton) was used to measure cellular GTP-RhoA. GTP-RhoA was precipitated from the cell lysates using rhotekin-RBD beads. The precipitated samples were analyzed by Western blotting with a RhoA monoclonal antibody.

Invasion Assay—The invasion assay was performed in triplicate in wells of a 24-well Transwell plate with an 8-μm pore size membrane (32). The membranes of the Transwell inserts were coated with type I collagen (2.5 μg/well, BD Biosciences). Cells (1×10^5/well) were placed into DMEM (0.1 ml) in the upper chamber. The 10% FBS-containing DMEM (used as a chemoattractant, 0.6 ml) was placed in the lower chamber. Serum-free DMEM (0.6 ml) was used as a control. Cells were allowed to invade for 4 h. The cells were stained for 10 min with 0.2% crystal violet/20% methanol (0.3 ml). The cells on the upper membrane surface were removed with a cotton swab. The dye from the cells that migrated onto the lower surface of the membrane was extracted with 1% SDS (0.25 ml). The resulting $A_{570\ nm}$ was measured using a plate reader.

Gelatin Substrate Zymography of MMP-2 and Western Blotting of RhoA, PTK7, and MT1-MMP—Basic protocols for these techniques have been described previously (29). The purified MMP-2 proenzyme (100 ng/ml) was added to MCF7 cells 12–14 h prior to the gelatin zymography analysis (35). For the Western blotting analysis of sPTK7, cells were incubated for 16 h in serum-free DMEM (20 ml/15-cm dish). The medium was then collected and concentrated 50-fold using Amicon Ultra-15 centrifugal filter units with a 30-kDa cutoff (Millipore). The concentrated samples (20 μl each) were used in Western blotting with a PTK7 antibody.

Modeling of the PTK7 and chz Structures—The three-dimensional structure of PTK7 was modeled by threading the PTK7 peptide sequence on the known structures of the homologues using MODWEB software (36, 37). The six N-terminal Ig domains of PTK7 (residues 28–588) were built using titin (PDB code 3B43) as a template. Because of their high (38%) sequence identity, the seventh Ig domain of PTK7 (residues 594–684) was built using the 22–105 fragment of Kiaa1556 (PDB code 2DM7). The 703–778 transmembrane region and the 789–1072 kinase domain of PTK7 were built using Hla (PDB code 1SYS) and a 258–525 fragment of Src (PDB code 2BDF; 38% sequence identity), respectively. The modeled fragment structures were merged to generate the structural model of PTK7 and *chz*. The structure of the catalytic domain of MT1-MMP was derived directly from PDB codes 1BQQ and 1BUV. The structures were then visualized using PyMOL software (DeLano Scientific).

RESULTS

PTK7 and chz Modeling—To visualize the structure of *chz*, we modeled the three-dimensional structures of PTK and *chz* (Fig. 1). Our structural modeling suggests that the conventional MT1-MMP PKP^{621} ↓ LI cleavage site is localized in the seventh Ig-like domain of PTK7. The Ala-Asn-Pro insertion that potentially results in the creation of the additional Pro-Glu-Lys ↓ Leu-Lys^{503} MMP cleavage site in the *chz* mutant sequence is localized in the junction region between the fifth and the sixth Ig-like domains.

The original QVLEKLK^{503} PTK7 sequence does not appropriately fit into the catalytic cleft of the MT1-MMP catalytic domain. In contrast, the QVLANPEK ↓ LK^{503} *chz* mutant sequence matches well the structural parameters of the active site cleft of MT1-MMP. The P1′ Leu-502 of the putative

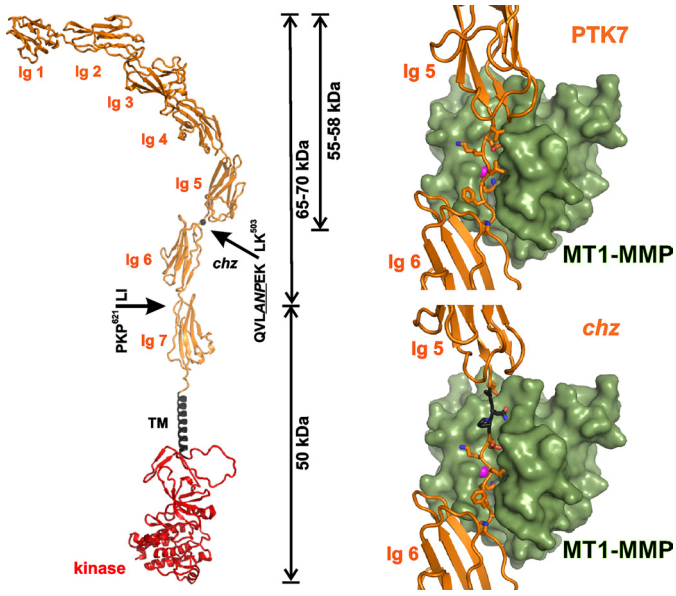

FIGURE 1. **A structure model of the full-length membrane PTK7.** *Left panel,* Ig domains 1–7, the transmembrane (*TM*), and kinase domains are shown in *orange*, *black*, and *red*, respectively. Cleavage of the PKP^{621} ↓ LI sequence in the seventh Ig-like domain and of the QVLANPEK ↓ LK^{503} *chz* in the junction region between the fifth and the sixth Ig-like domains, respectively, is shown by the *arrows*. The mutant residues are *underlined*. *Right panel,* a structural model of the QVLEK ↓ LK^{503} original PTK7 and the QVLANPEK ↓ LK^{503} *chz* mutant sequences in the catalytic cleft of the MT1-MMP catalytic domain. *Green*, MT1-MMP; *orange*, PTK7/*chz*; *black*, Ala-Asn-Pro insert in *chz*; *magenta ball*, active site zinc.

Lys-Leu scissile bond appears proximal to the active site zinc (Fig. 1).

Cell Surface chz Is Efficiently Degraded—To determine the expression levels and potential link of PTK7 with MT1-MMP, the FLAG-tagged PTK7 and *chz* constructs were designed. Breast carcinoma MCF-7 cells were stably transfected with the wild-type PTK7 and *chz* constructs. In addition, PTK7 and *chz* were coexpressed in MCF-7 cells with the wild-type MT1-MMP and the catalytically inactive E240A MT1-MMP mutant (MCF7-MT1 and MCF7-E240A cells, respectively). To facilitate the identification of MT1-MMP, the proteinase constructs were tagged with a V5 tag. We specifically selected MCF7 cells for our studies because the parental cell line is deficient in MT1-MMP (38). As expected, gelatin zymography of the medium aliquots confirmed the ability of MCF7-MT1 cells to transform the proenzyme of MMP-2 into the activated MMP-2 forms, whereas parental MCF7 cells and MCF7-E240 cells were inactive in this assay (Fig. 2*A*).

Cells were surface-biotinylated and then lysed. Both biotin-labeled, cell surface-associated *chz* and MT1-MMP were precipitated using streptavidin beads. Cells expressing PTK7 were used as controls in our experiments. The precipitated *chz* and MT1-MMP samples were analyzed by Western blotting with the FLAG and V5 antibodies, respectively. MT1-MMP was represented by the enzyme form on the surface of MCF7-E240A and MCF7-MT1 cells. The latter also exhibited the 45-kDa self-proteolysis degradation form that was absent in MCF7-E240 cells. The levels of cell surface *chz* inversely correlated with the cell surface MT1-MMP activity. Thus, minor levels of *chz* as compared with PTK7 were detected on the surface of MCF7-MT1 cells (Fig. 2*A*).

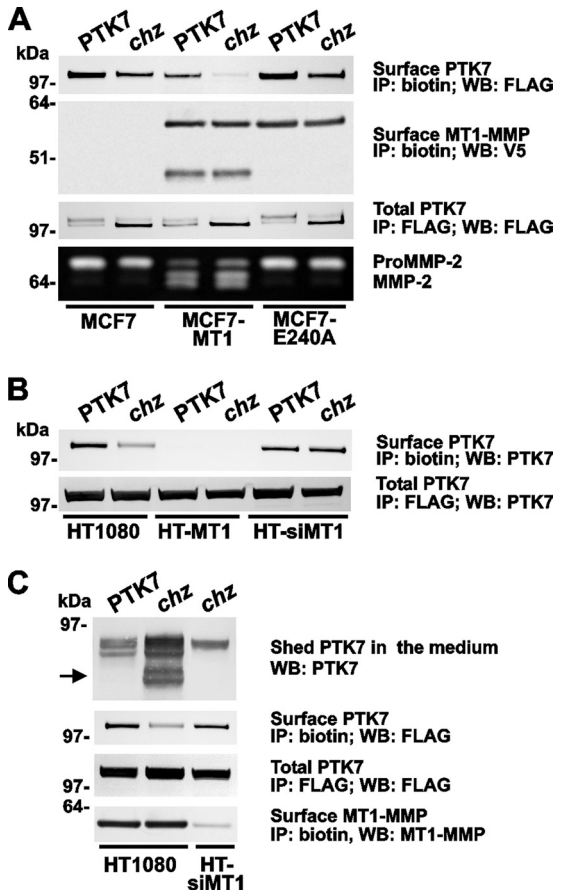

FIGURE 2. ***Chz* is efficiently cleaved by MT1-MMP.** *A*, cell surface, biotin-labeled, and total cell lysate immunoprecipitated samples (surface and total, respectively) of MCF7 cells expressing the FLAG-tagged PTK7/*chz* constructs and of MCF7-MT1 and MCF7-E240 cells that coexpressed the FLAG-tagged PTK7/*chz* constructs with the V5-tagged MT1-MMP and the catalytically inert E240 MT1-MMP mutant constructs, respectively, were analyzed by Western blotting. *Bottom panel*, the ability of cellular MT1-MMP to activate the added MMP-2 proenzyme (100 ng/ml) was analyzed with gelatin zymography. *B*, cell surface, biotin-labeled, and total cell lysate samples (surface and total, respectively) of HT1080, HT-MT1, and HT-siMT1 cells expressing the FLAG-tagged PTK7/*chz* constructs were analyzed by Western blotting. *C*, conditioned medium aliquots and cell surface, biotin-labeled, and total cell lysate immunoprecipitated samples (surface and total, respectively) of HT1080 cells expressing the FLAG-tagged PTK7/*chz* constructs and of HT-siMT1 cells expressing the FLAG-tagged *chz* construct were analyzed by Western blotting. Equal amounts of total protein (50 μg/lane) were analyzed in *A*, *B*, and *C*. The *arrow* indicates the abnormal cleavage product in *chz*. *IP*, immunoprecipitation with the FLAG antibody and streptavidin beads. *WB*, Western blotting with the FLAG, V5, PTK7, and MT1-MMP antibodies. For the beads and antibodies used, see *panel labels*.

To corroborate these data, we determined the levels of total cellular PTK7 and *chz* in MCF7, MCF7-MT1, and MCF7-E240A cells (Fig. 2*A*). For these purposes, cells were lysed, and *chz* was pulled down from the cell extracts using the FLAG antibody beads. The precipitates were analyzed by Western blotting with the FLAG antibody. The *chz* construct was efficiently synthesized by MCF7, MCF7-MT1, and MCF7-E240A. The presence of the two isoforms of PTK7/*chz* we observed in the cell extracts is not precisely clear as of now. The levels of cellular *chz* exceeded those of PTK7 in all three lines. The cell surface levels of *chz*, however, were low, especially in MCF7-MT1 cells.

These results suggest the existence of the efficient degradation of cell surface *chz* rather than the low synthesis of *chz* by the cells and that this degradation of cell surface *chz* is MT1-MMP-dependent. Because breast carcinoma MCF7 cells do not efficiently invade the matrix layers *in vitro*, it is exceedingly difficult to observe the effects of PTK7, *chz*, and MT1-MMP on the invasion of this cell type.

To support our data further and to determine the potential effect of PTK7 and *chz* on cell invasion, we employed highly migratory and invasive fibrosarcoma HT1080 cells, which synthesize MT1-MMP naturally. First, we determined the status of cellular *chz* in HT1080 cells. As controls, we used HT-siMT1 cells with the transcriptional silencing of MT1-MMP and also HT-MT1 cells with the forced expression of MT1-MMP (Fig. 2*B*). To measure cell surface *chz*, the cells were surface-biotinylated and lysed. Biotin-labeled material was captured using streptavidin beads. To determine the total cell *chz*, untreated cells were lysed, and the FLAG-tagged constructs were captured on FLAG antibody beads. Both biotin-labeled and total cell samples were then analyzed by Western blotting with the antibody against the PTK7 ectodomain. There was no difference in the levels of total PTK7 and *chz* in HT1080, HT-MT1, and HT-siMT1 cells. Cell surface *chz* was diminished in HT1080 cells as compared with PTK7. Both PTK7 and *chz* were predominantly shed by MT1-MMP activity in HT-MT1 cells. As a result, there was no detectable PTK7 and *chz* in the HT-MT1 cell surface samples. Transcriptional knockout of MT1-MMP restored the cell surface PTK7 and *chz* in HT-siMT1 cells.

In agreement, as detected by Western blotting with the FLAG antibody, there was no difference in the total levels of cellular PTK7 and *chz* in HT1080 and HT-siMT1 cells. Consistent with other assays, minor cell surface levels of *chz* were observed in HT1080 cells as compared with PTK7. The surface levels of *chz* significantly increased in HT-siMT1 cells. Because MT1-MMP is a principal sheddase of membrane PTK7 (29), we also assessed the levels of the shed *chz* ectodomain in the concentrated medium samples using Western blotting with the PTK7 antibody. MT1-MMP proteolysis released the soluble, 65- to 70-kDa PTK7 1–621 ectodomain into the medium (Fig. 2*C*). As compared with PTK7, extensive shedding of *chz* was observed in HT1080 cells. This shedding was greatly diminished in HT-siMT1 cells. The presence of the additional, low molecular weight fragments (55–58 kDa) of *chz* directly supported the presence of the additional MT1-MMP cleavage site in the ectodomain sequence. The molecular mass of these fragments (55–58 kDa) correlated with the expected size of the N-terminal, 1–500 proteolytic fragment of *chz*.

To visualize the relations between *chz* and MT1-MMP, we immunostained the permeabilized HT1080, HT-MT1, and HT-siMT1 cells using the PTK7 antibody (Fig. 3). There was an abundant immunoreactivity of both PTK7 and especially *chz* in the plasma membrane and intracellular compartments of HT-siMT1 cells. In turn, in HT1080 cells, only PTK7 but not *chz* was detected on the plasma membrane. Both PTK7 and *chz* were not detected on the plasma membrane in HT-MT1 cells, thus supporting the clearance of PTK7 and especially *chz* by the plasma membrane MT1-MMP activity. Immunostaining of actin revealed the rearrangements in the actin cytoskeleton in the cells we tested.

Chz Affects Cell Invasion—According our data and that of others, PTK7 is directly involved in the regulation of cell migration (29, 39–43). Cell surface levels of PTK7 appear to correlate inversely with tumor aggressiveness and metastatic potential (29). Because of these earlier data and because actin cytoskeleton dynamics are also associated with cell migration (44, 45), we next analyzed the invasive capacity of HT1080, HT-PTK7, HT-L622D, HT-sPTK7, HT-*chz*, and HT-siMT1/*chz* cells.

Consistent with our earlier results (29), the ectopic expression of PTK and especially the uncleavable L622D PTK7 mutant suppressed cell migration (Fig. 4). On the contrary, the expression of *chz* enhanced cell migration ~2-fold relative to the original, highly migratory HT1080 cells. In HT-siMT1 cells, the stimulatory effect of *chz* was not observed, again suggesting the presence of a link between MT1-MMP activity and the *chz* functionality.

To shed more light on the effects of *chz*, we determined the activation status of cellular RhoA GTPase (Fig. 4). In agreement with our previous observations (29), only the HT-sPTK7 and original HT1080 cells exhibited significant levels of activated GTP-RhoA. In other cells we tested, including HT-*chz* and HT-siMT1/*chz*, the GTP-RhoA levels were similarly low. On the basis of these results, we suggest that GTP-Rho is not critical for the yet to be determined PTK7 pathway that drives cell locomotion.

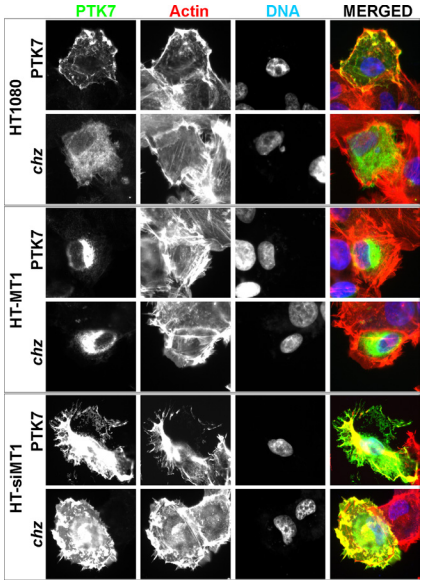

FIGURE 3. **Immunoreactivity of PTK7 and *chz* in HT1080 cells.** Staining of HT1080, HT-MT1, and HT-siMT1 cells expressing the PTK7/*chz* constructs using the PTK7 antibody (*green*) and phalloidin (actin, *red*). *Blue*, nuclei (DAPI).

DISCUSSION

Ubiquitously expressed PTK7 pseudo-kinase is an essential component of the non-canonical Wnt/PCP signaling pathway, arguably one of the most important cellular pathways in eukaryotes (46, 47). At its most basic level, polarity may be considered as the generation of asymmetry within a single cell, whether the result of the asymmetry is a directed movement that leads to cellular migration or to the relocalization of specific multicellular structures. The nature of its specific binding partners and the multifunctional role of PTK7 in cell migration are yet to be elucidated. It is likely that in different cell systems, PTK7 is involved in the interactions with Plexin1 (41), receptor for activated protein kinase C (RACK1) (40), vascular endothelial growth factor receptor 1 (FLT-1) (39), disheveled (dsh) (43), Van Gogh-like 2 (VANGL2) (17, 30) and β-catenin (48).

Polarized cell locomotion also correlates well with pericellular proteolysis and extracellular matrix remodeling, both of which involve the action of MT1-MMP (49–51). Our results suggest that the Wnt/PCP pathway and pericellular proteolysis converge at PTK7 to promote efficient directed cell migration both in normal development and cancer (29).

PTK7 is a major cleavage target of MT1-MMP in the plasma membrane. MT1-MMP directly cleaves the PKP$^{621}\downarrow$LI sequence in an exposed region of PTK7, generating the N-terminal, soluble PTK7 ectodomain. Because PTK7 readily oligomerizes through its ectodomain (10, 52), membrane PTK7 forms a complex either with itself or with the solubilized ectodomain or with some yet to be identified adaptor protein(s) (2, 13, 39–41, 43, 48). It is likely that these different complex types elicit the dissimilar downstream signaling events and that these signaling events differentially regulate multiple cell functions, including PCP and directional motility, in processes as diverse as cancer cell invasion and embryonic cell migration during gastrulation in eukaryotes (13, 18, 28, 30). In agreement, the soluble PTK7 ectodomain inhibited angiogenesis *in vitro* and *in vivo* in a dominant-negative fashion by competing with full-length PTK7 (12). As a result, the ratio between the soluble and the membrane PTK7 appears to be an important factor in the Wnt/PCP regulation. The importance of PTK7 is also illustrated by the fact that PTK7 mutant mice that express a 1–114 PTK7 trunca-

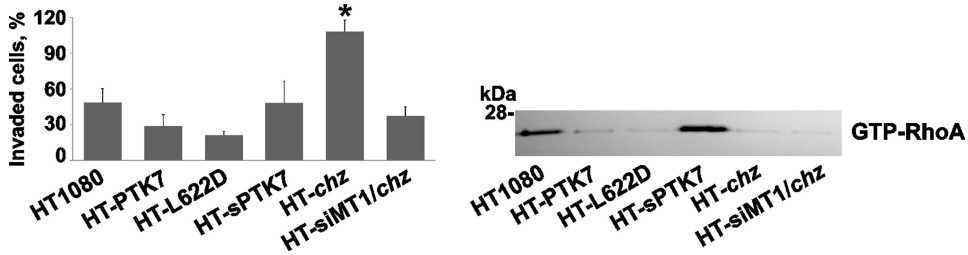

FIGURE 4. ***chz* stimulates cell invasion but does not activate GTP-RhoA.** *Left panel*, cell invasion through a type 1 collagen matrix by HT1080 cells transfected with the indicated MT1-MMP and PTK7/*chz* constructs. FBS (10%) was used as a chemoattractant. The *error bars* represent mean ± S.D. *, $p < 0.05$. The experiments were repeated multiple times with comparable results. *Right panel*, GTP-RhoA pull-down assay in HT1080 cells transfected with the indicated MT1-MMP and PTK7/*chz* constructs. The samples (1 mg of total protein each) were precipitated using rhotekin beads. The precipitates were analyzed by Western blotting with the RhoA antibody.

tion die perinatally because of severe defects in neural tube closure. Overexpression of the mutant PTK7 lacking its cytoplasmic domain resulted in similar abnormalities (10).

From these perspectives, identification of the *chz* PTK7 mutant represents a step forward to a better understanding of PTK7 functionality. The *chz* mutation results in the Ala-Asn-Pro insertion into the PTK7 sequence and causes a significant reduction in membrane localization of the PTK7 protein (17). Our experimental results firmly determined that the three-amino-acid insert incorporated an additional MT1-MMP cleavage site into the PTK7 ectodomain. In fact, because of the *chz* mutation, the consensus P*XX* ↓ L MMP cleavage site is reconstituted in the PTK7 protein. Regardless of the primary importance of MT1-MMP in the cleavage of *chz*, however, it cannot be ruled out that certain additional soluble and membrane-type MMPs also contribute to the aberrant cleavage of *chz* in other cells/tissue systems.

It is now clear that because of the aberrant MT1-MMP proteolysis, the soluble N-terminal 1–621 70-kDa fragment is unstable in *chz*. In a model migration system, the forced expression of *chz* significantly stimulated cancer cell invasion. Accordingly, it is now tempting to hypothesize that *chz* affected the precisely balanced, polarized, directed cell movement in the course of gastrulation in mice and that these aberrations in shaping the body plan resulted in the multiple phenotypic defects in the *chz* mutant animals (17).

Intriguingly, the forced expression of the soluble PTK7 1–700 ectodomain but not of *chz* significantly up-regulated cellular GTP-RhoA, suggesting that the invasion-promoting function of *chz* does not require RhoA activity.

Taken together, our novel data in a combination with our results and those of others (17, 18, 28, 29) imply that the MT1-MMP/PTK7 axis plays an important role in multiple cell locomotion situations, including morphogenetic cell movements, that shape the body plan and that the aberrations of either of MT1-MMP or PTK7 or both in gastrulation may result in multiple developmental diseases, including congenital defects. Accordingly, we believe that further studies into the MT1-MMP and PTK7 roles in PCP and their potential link to diseases such as birth defects are warranted to design a means for birth defect prognostics and correction.

REFERENCES

1. Simons, M., and Mlodzik, M. (2008) *Annu. Rev. Genet.* **42,** 517–540
2. Katoh, M. (2005) *Oncol. Rep.* **14,** 1583–1588
3. Roszko, I., Sawada, A., and Solnica-Krezel, L. (2009) *Semin. Cell Dev. Biol.* **20,** 986–997
4. Dale, T. C. (1998) *Biochem. J.* **329,** 209–223
5. Yin, C., Ciruna, B., and Solnica-Krezel, L. (2009) *Curr. Top. Dev. Biol.* **89,** 163–192
6. Goodrich, L. V. (2008) *Neuron* **60,** 9–16
7. Grassot, J., Gouy, M., Perrieèe, G., and Mouchiroud, G. (2006) *Mol. Biol. Evol.* **23,** 1232–1241
8. Jung, J. W., Ji, A. R., Lee, J., Kim, U. J., and Lee, S. T. (2002) *Biochim. Biophys. Acta* **1579,** 153–163
9. Jung, J. W., Shin, W. S., Song, J., and Lee, S. T. (2004) *Gene* **328,** 75–84
10. Lu, X., Borchers, A. G., Jolicoeur, C., Rayburn, H., Baker, J. C., and Tessier-Lavigne, M. (2004) *Nature* **430,** 93–98
11. Park, S. K., Lee, H. S., and Lee, S. T. (1996) *J. Biochem.* **119,** 235–239
12. Shin, W. S., Maeng, Y. S., Jung, J. W., Min, J. K., Kwon, Y. G., and Lee, S. T. (2008) *Biochem. Biophys. Res. Commun.* **371,** 793–798
13. Yen, W. W., Williams, M., Periasamy, A., Conaway, M., Burdsal, C., Keller, R., Lu, X., and Sutherland, A. (2009) *Development* **136,** 2039–2048
14. Mossie, K., Jallal, B., Alves, F., Sures, I., Plowman, G. D., and Ullrich, A. (1995) *Oncogene* **11,** 2179–2184
15. Whitford, K. L., and Ghosh, A. (2001) *Neuron* **32,** 1–3
16. Toyofuku, T., Zhang, H., Kumanogoh, A., Takegahara, N., Suto, F., Kamei, J., Aoki, K., Yabuki, M., Hori, M., Fujisawa, H., and Kikutani, H. (2004) *Genes Dev.* **18,** 435–447
17. Paudyal, A., Damrau, C., Patterson, V. L., Ermakov, A., Formstone, C., Lalanne, Z., Wells, S., Lu, X., Norris, D. P., Dean, C. H., Henderson, D. J., and Murdoch, J. N. (2010) *BMC Dev. Biol.* **10,** 87
18. Coyle, R. C., Latimer, A., and Jessen, J. R. (2008) *Exp. Cell Res.* **314,** 2150–2162
19. Egeblad, M., and Werb, Z. (2002) *Nat. Rev. Cancer* **2,** 161–174
20. Itoh, Y. (2006) *IUBMB Life* **58,** 589–596
21. Morrison, C. J., Butler, G. S., Rodríguez, D., and Overall, C. M. (2009) *Curr. Opin. Cell Biol.* **21,** 645–653
22. Rodríguez, D., Morrison, C. J., and Overall, C. M. (2010) *Biochim. Biophys. Acta* **1803,** 39–54
23. Strongin, A. Y. (2010) *Biochim. Biophys. Acta* **1803,** 133–141
24. Hotary, K., Li, X. Y., Allen, E., Stevens, S. L., and Weiss, S. J. (2006) *Genes Dev.* **20,** 2673–2686
25. Sabeh, F., Ota, I., Holmbeck, K., Birkedal-Hansen, H., Soloway, P., Balbin, M., Lopez-Otin, C., Shapiro, S., Inada, M., Krane, S., Allen, E., Chung, D., and Weiss, S. J. (2004) *J. Cell Biol.* **167,** 769–781
26. Holmbeck, K., Bianco, P., Caterina, J., Yamada, S., Kromer, M., Kuznetsov, S. A., Mankani, M., Robey, P. G., Poole, A. R., Pidoux, I., Ward, J. M., and Birkedal-Hansen, H. (1999) *Cell* **99,** 81–92
27. Golldack, D., Popova, O. V., and Dietz, K. J. (2002) *J. Biol. Chem.* **277,** 5541–5547
28. Jessen, J. R. (2009) *Zebrafish* **6,** 21–28
29. Golubkov, V. S., Chekanov, A. V., Cieplak, P., Aleshin, A. E., Chernov, A. V., Zhu, W., Radichev, I. A., Zhang, D., Dong, P. D., and Strongin, A. Y. (2010) *J. Biol. Chem.* **285,** 35740–35749
30. Cantrell, V. A., and Jessen, J. R. (2010) *Cancer Lett.* **287,** 54–61
31. Golubkov, V. S., Boyd, S., Savinov, A. Y., Chekanov, A. V., Osterman, A. L., Remacle, A., Rozanov, D. V., Doxsey, S. J., and Strongin, A. Y. (2005) *J. Biol. Chem.* **280,** 25079–25086
32. Golubkov, V. S., Chekanov, A. V., Savinov, A. Y., Rozanov, D. V., Golubkova, N. V., and Strongin, A. Y. (2006) *Cancer Res.* **66,** 10460–10465
33. Rozanov, D. V., Savinov, A. Y., Williams, R., Liu, K., Golubkov, V. S., Krajewski, S., and Strongin, A. Y. (2008) *Cancer Res.* **68,** 4086–4096
34. Sounni, N. E., Rozanov, D. V., Remacle, A. G., Golubkov, V. S., Noel, A., and Strongin, A. Y. (2010) *Int. J. Cancer.* **126,** 1067–1078
35. Golubkov, V. S., Cieplak, P., Chekanov, A. V., Ratnikov, B. I., Aleshin, A. E., Golubkova, N. V., Postnova, T. I., Radichev, I. A., Rozanov, D. V., Zhu, W., Motamedchaboki, K., and Strongin, A. Y. (2010) *J. Biol. Chem.* **285,** 27726–27736
36. Eswar, N., Eramian, D., Webb, B., Shen, M. Y., and Sali, A. (2008) *Methods Mol. Biol.* **426,** 145–159
37. Pieper, U., Eswar, N., Webb, B. M., Eramian, D., Kelly, L., Barkan, D. T., Carter, H., Mankoo, P., Karchin, R., Marti-Renom, M. A., Davis, F. P., and Sali, A. (2009) *Nucleic Acids Res.* **37,** D347–354
38. Deryugina, E. I., Bourdon, M. A., Jungwirth, K., Smith, J. W., and Strongin, A. Y. (2000) *Int. J. Cancer* **86,** 15–23
39. Lee, H. K., Chauhan, S. K., Kay, E., and Dana, R. (2011) *Blood* (in press)
40. Wehner, P., Shnitsar, I., Urlaub, H., and Borchers, A. (2011) *Development* **138,** 1321–1327
41. Wagner, G., Peradziryi, H., Wehner, P., and Borchers, A. (2010) *Biochem. Biophys. Res. Commun.* **402,** 402–407
42. Prebet, T., Lhoumeau, A. C., Arnoulet, C., Aulas, A., Marchetto, S., Audebert, S., Puppo, F., Chabannon, C., Sainty, D., Santoni, M. J., Sebbagh, M., Summerour, V., Huon, Y., Shin, W. S., Lee, S. T., Esterni, B., Vey, N., and Borg, J. P. (2010) *Blood* **116,** 2315–2323
43. Shnitsar, I., and Borchers, A. (2008) *Development* **135,** 4015–4024
44. Parsons, J. T., Horwitz, A. R., and Schwartz, M. A. (2010) *Nat. Rev. Mol. Cell Biol.* **11,** 633–643

45. Ridley, A. J., Schwartz, M. A., Burridge, K., Firtel, R. A., Ginsberg, M. H., Borisy, G., Parsons, J. T., and Horwitz, A. R. (2003) *Science* **302,** 1704–1709
46. Neth, P., Ries, C., Karow, M., Egea, V., Ilmer, M., and Jochum, M. (2007) *Stem Cell Rev.* **3,** 18–29
47. Polakis, P. (2000) *Genes Dev.* **14,** 1837–1851
48. Puppo, F., Thomé, V., Lhoumeau, A. C., Cibois, M., Gangar, A., Lembo, F., Belotti, E., Marchetto, S., Lécine, P., Prébet, T., Sebbagh, M., Shin, W. S., Lee, S. T., Kodjabachian, L., and Borg, J. P. (2011) *EMBO Rep.* **12,** 43–49
49. Wolf, K., and Friedl, P. (2009) *Clin. Exp. Metastasis* **26,** 289–298
50. Itoh, Y., and Seiki, M. (2006) *J. Cell. Physiol.* **206,** 1–8
51. Seiki, M., and Yana, I. (2003) *Cancer Sci.* **94,** 569–574
52. Pulido, D., Campuzano, S., Koda, T., Modolell, J., and Barbacid, M. (1992) *EMBO J.* **11,** 391–404